

# Rotation and flares of M dwarfs with habitable zones accessible to TESS

M. Bogner<sup>1,\*</sup>, B. Stelzer<sup>1,2</sup> and St. Raetz<sup>1</sup>

[1] Institut für Astronomie und Astrophysik Tübingen (IAAT) [2] INAF – Osservatorio Astronomico di Palermo [\*] bogner@astro.uni-tuebingen.de

## Sample

- **112 M dwarfs** (spectral types K8 to M5)
- listed in TESS Habitable Zone Star Catalog (Kaltenegger+2019)
- TESS can **detect planets in the full extent of the habitable zone**
- TESS  $\text{mag} \leq 11.5$
- **1276 2-min. cadence light curves** (LCs) analyzed; example LC in Fig. 1

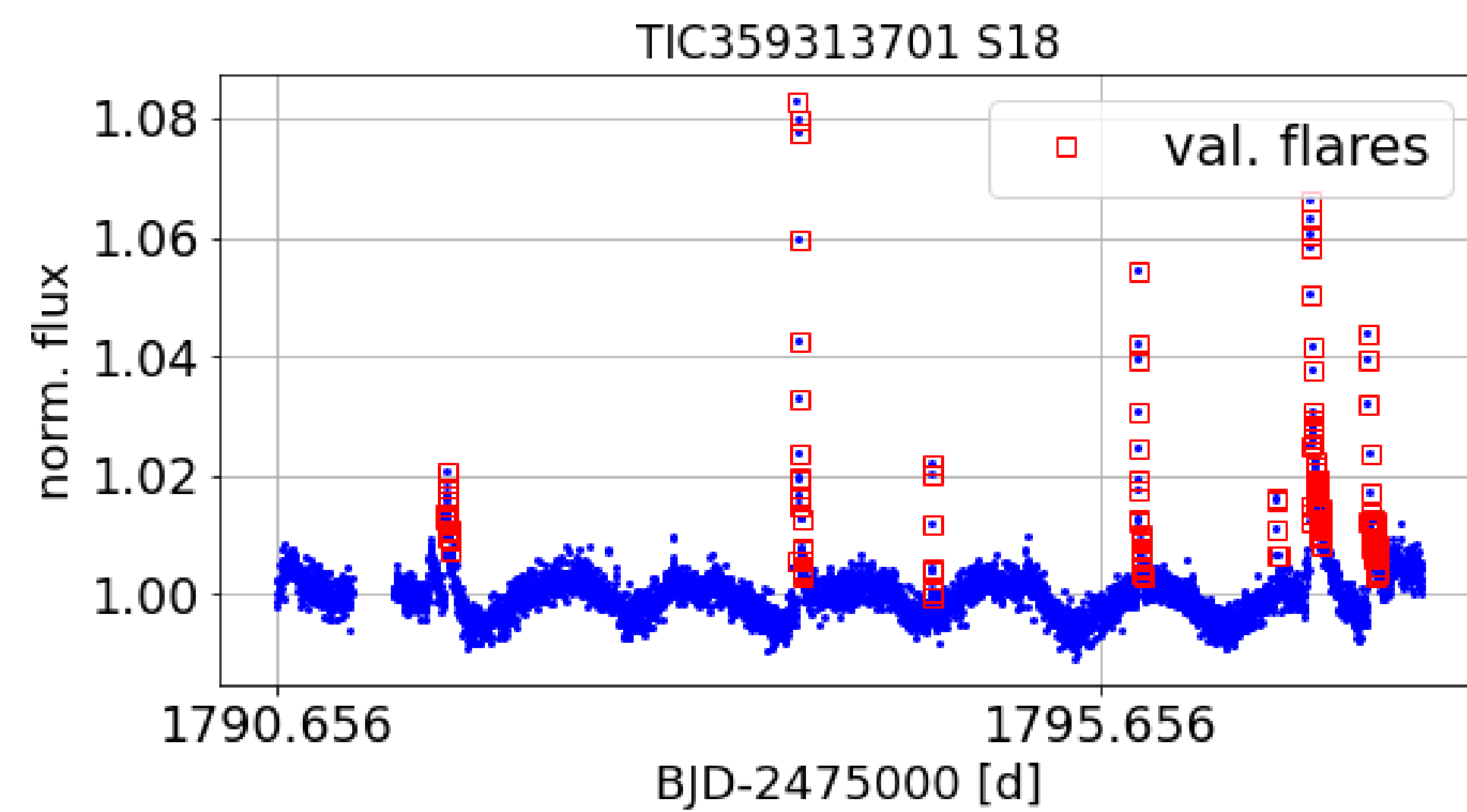


Fig. 1: Example of a TESS light curve showing rotational modulation (blue) and flares (red).

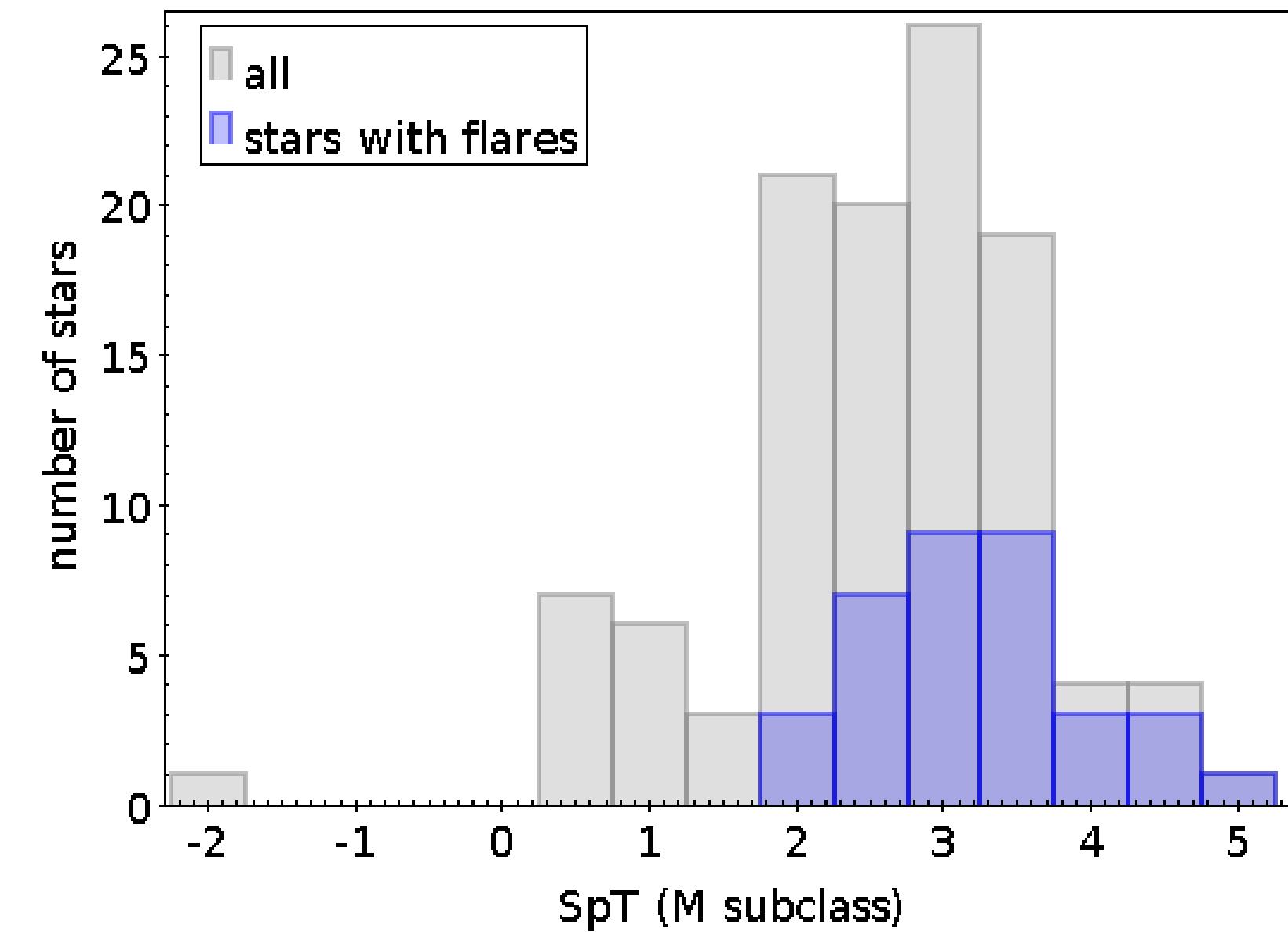


Fig. 2: Spectral type distribution of our sample. Numbers denote M subclasses, -2 stand for K8. (Bogner et al., in prep.)

## Data Analysis

For details, see Stelzer+2016 and Raetz+2020



The algorithm can be briefly summarized as follows:

- **rotation period search** with 3 methods: Generalized Lomb Scargle Periodogram, autocorrelation function and sine fit
- **flare detection** based on flattened and cleaned LC with standard deviation  $S_{\text{flat}}$ : A **potential flare** is a part of the original LC with **3 or more consecutive data points deviating  $> 3 S_{\text{flat}}$**  from the LC's mean value.
- further **validation criteria** (e. g. decay time  $>$  rise time)
- **contamination factor** =  $\frac{\text{summed up flux of contaminating stars in aperture mask}}{\text{target flux}}$
- **energy completeness limit for flare detection** determined from flare energy frequency distribution (FFD) following Hawley+2014

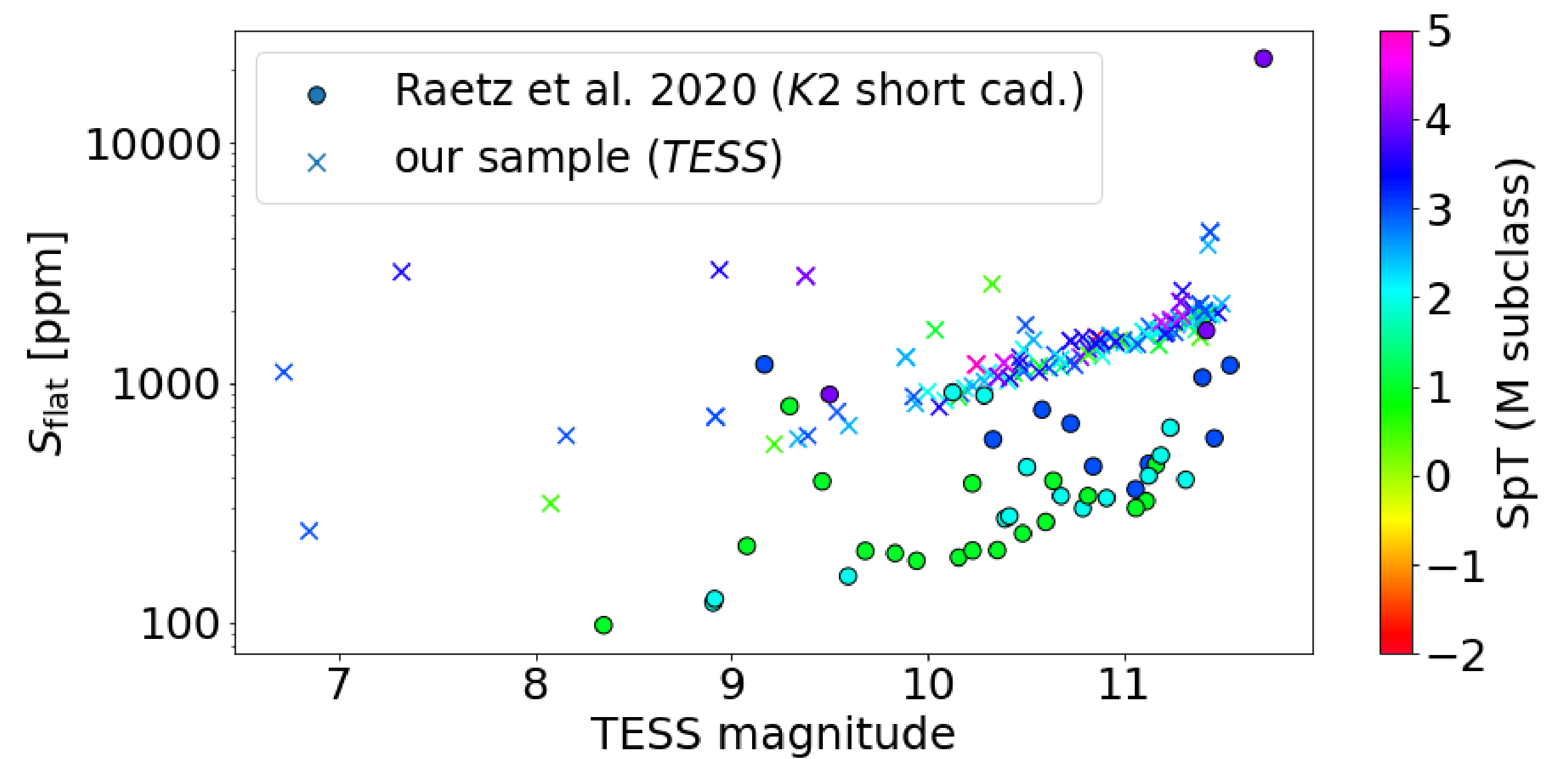


Fig. 3: Standard deviation of the flattened and cleaned LC as a function of TESS magnitude. For comparison, the values of K2 short cadence LCs from Raetz+2020 are also shown. The figure makes use of an empirical conversion between K2 and TESS magnitudes that we derived based on  $\sim 19\,000$  main-sequence stars. (Bogner et al., in prep.)

## Analysis results

- **35 stars** show flares ( $\sim 31\%$  of the sample); **2532 flares** detected
- **fraction of flaring stars higher for later M SpT subclasses** (cf. Fig. 2)
- **12 stars** ( $\sim 11\%$  of the sample) show **reliable rotation periods** (i. e. period search yielded consistent results for all TESS sectors of the star)
- rotational modulations with low amplitudes are hidden in the noise for **TESS LCs** due to **higher standard deviation w. r. t. K2** (Fig. 3)
- **$0.28 \text{ d} \leq P_{\text{rot}} \leq 3.94 \text{ d}$**
- 2138 flares occur on the 12 stars with reliable  $P_{\text{rot}}$  - only 394 flares on others
- for most flares: **peak flare flux at inner HZ boundary** is larger than the bolometric flux hitting the top of Earth's atmosphere, i. e.  **$(\text{peak flare flux})/S_0 > 1$** , cf. Fig. 4
- binned flare energy frequency distribution (FFD) for earlier SpT range (M2.5-M3.5) shifted to higher flare energies w.r.t. later SpT range (M4.5-M5) (Fig. 5)  
→ **flares on later M subtype stars are less energetic**
- stars with higher flare rates have higher energies of their largest flares; **stars with reliable  $P_{\text{rot}}$  have the highest flare rates** (Fig. 6)

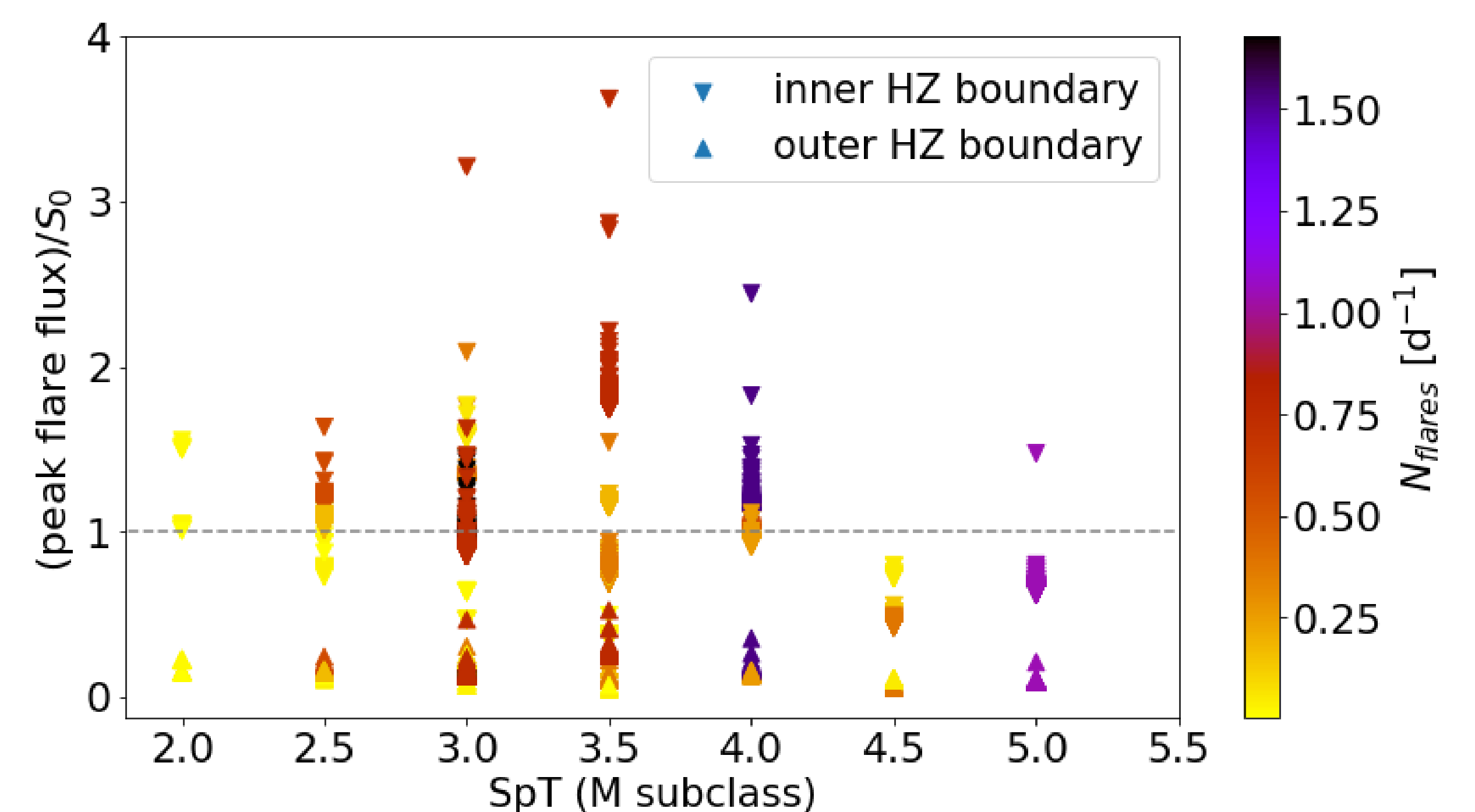


Fig. 4: Peak flare flux at the inner (Recent Venus) and outer (Early Mars) habitable zone boundary. Fluxes are normalized by the solar constant. The flare rate of each star is color-coded.

## Summary

- rotational modulation with low amplitude difficult to detect with TESS due to high standard deviation of the LCs (Fig. 3)
- atmospheres of potential exoplanets at inner HZ boundary are exposed to larger fluxes during flare events than Earth in quiescent solar state (Fig. 4)
- earlier M subtype stars show flares with higher energies (Fig. 5)
- stars with reliable  $P_{\text{rot}}$  show higher flare rates; for each SpT, stars with higher flare rates also show higher energies of their largest flare (Fig. 6)

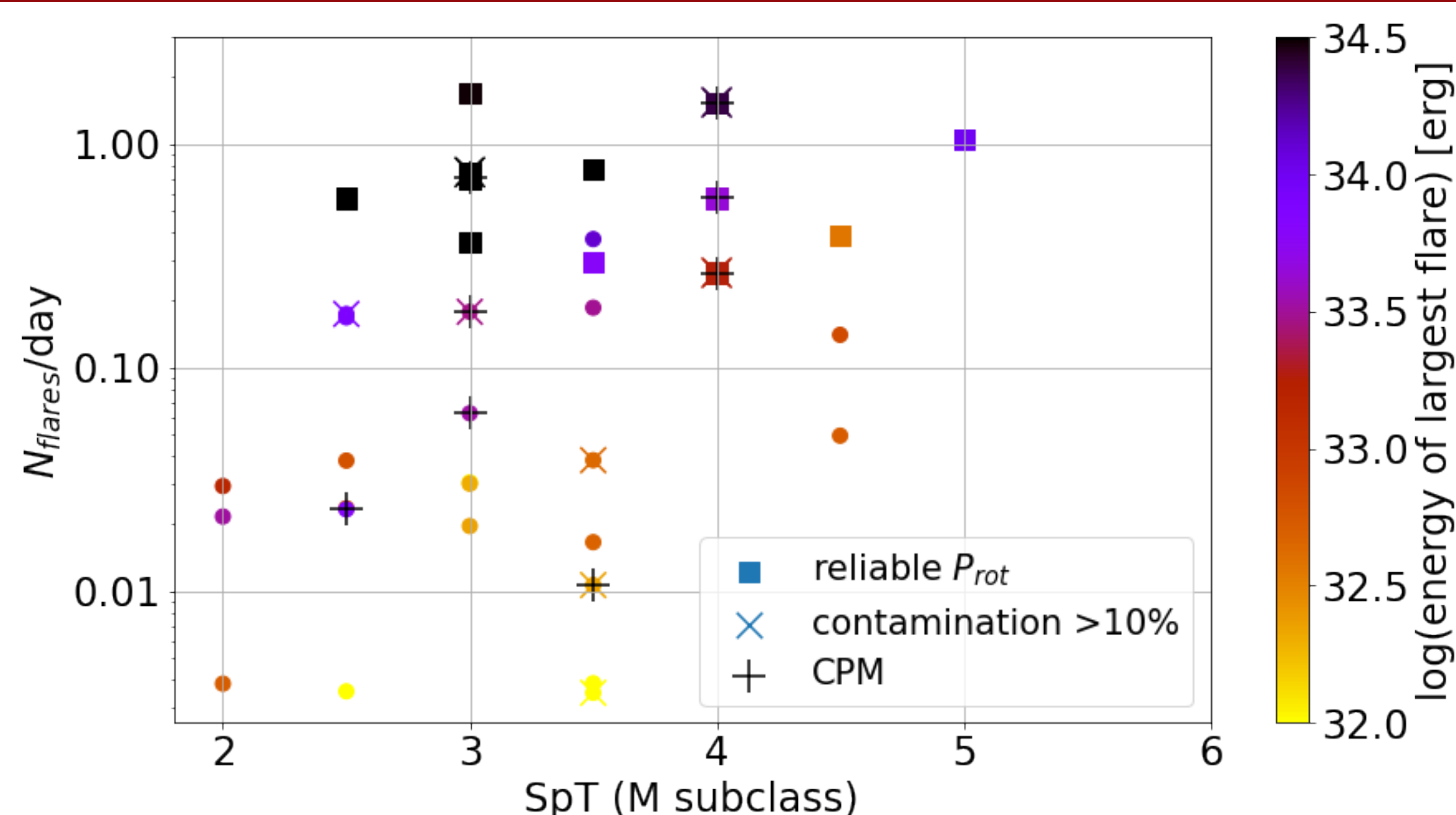


Fig. 6: Relation btw. flare rate and SpT. Stars in binaries are marked with '+', 'x' denotes those with a flux contamination  $> 10\%$ .

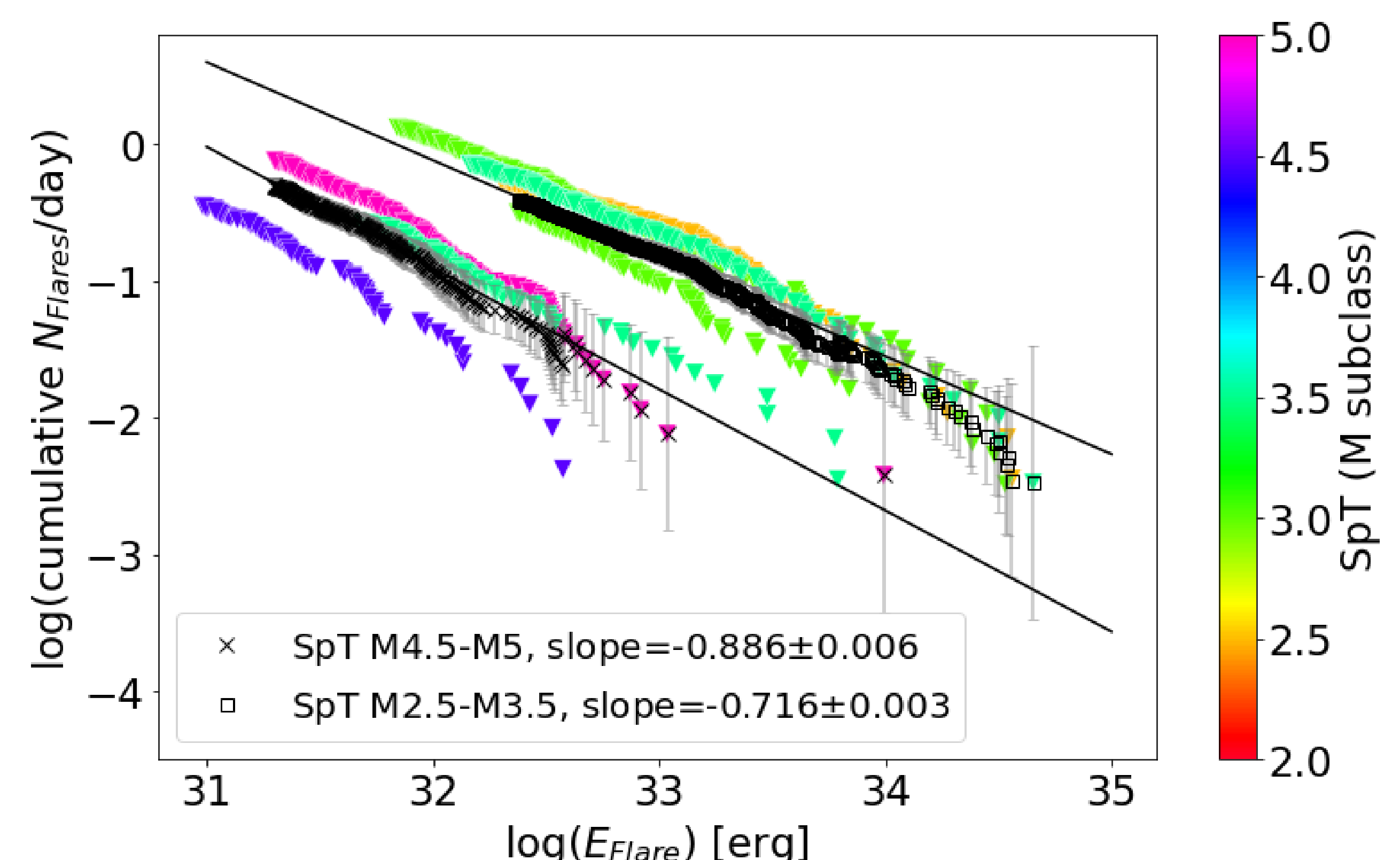


Fig. 5: FFDs of the 7 stars with reliable rotation periods that are not part of a close binary and have a flux contamination factor  $< 10\%$ . Only data points above the energy detection threshold are plotted. Black curves: binned FFDs in two different SpT ranges and fits. (Bogner et al., in prep.)